International Journal of Energy
ISSN: 2957-9473 | Vol. 3, No. 1, 2023

Research on Structural Design and Optimization of Battery Thermal Management System

Lin Xi *, Haoxiang Zhang, Mengxi Gao, Xiao Luo, Longjie Wang, Qian Wang

School of Automotive Engineering, Geely University, Chengdu 641423, China

*** Corresponding author:** Lin Xi (Email: 1923878906@qq.com)

Abstract: The quality of the thermal management control strategy of the power battery is directly related to the energy consumption and the use state of the battery. The lithium battery will generate heat in the process of charging and discharging, which will lead to its own temperature rise, and the temperature rise will affect the performance of the lithium battery. In this paper, the simulation analysis from the cell to the battery pack is carried out, and the thermal simulation analysis of the air-cooled and liquid-cooled battery pack is carried out by using different control strategies. This paper mainly analyzes the thermal simulation of three discharge rates of single lithium battery under normal temperature environment, and designs the type I liquid cooled battery pack and type S liquid cooled battery pack. By setting the same liquid cooling control strategy, the inlet temperature is 20°C, the flow rate is 1m/s, the initial temperature of the battery in normal temperature environment is 25°C, and the cooling medium is ethylene glycol (50% water and ethylene glycol mixture). Through simulation analysis and comparison of the heat dissipation effect under the three discharge ratios, the research results show that the maximum temperature of the type I liquid cooled battery pack is lower than that of the type S liquid cooled battery pack, and the effect is more significant.

Keywords: Thermal Management Control Strategy; Thermal Simulation Analysis; Type I Liquid Cooled Battery Pack; Model S Liquid Cooled Battery Pack.

1. Introduction

In the past 50 years, with the wide application of motor vehicles in human society, the wide application of motor vehicles not only makes the problem of fuel shortage in China more prominent, but also brings a series of problems such as the greenhouse effect caused by the increase of CO2 emissions. Continued emissions from conventionally fueled vehicles have led to melting snow in the Arctic, contributing to climate warming. All countries in the world are not only affected by serious environmental pollution and lack of resources, but also lack and difficult to exploit oil resources, and the high dependence on oil leads to a huge waste of oil resources and aggravates air pollution [1]. In the carbon neutral policy proposed by the state, and under the dual pressure of saving resources and protecting the environment, new energy electric vehicles have the advantages of clean energy, sustainable development of resources, and no pollutant emission. At present, new energy vehicles have begun to use combustible ice, wind energy, etc., and the most common should also be electric energy [2]. Therefore, all countries attach great importance to the research and development of new energy electric vehicles.

The development of new energy vehicles is the inevitable way for China to develop from an automobile power to an automobile power [3]. At present, China's new energy vehicles are mainly pure electric vehicles, fuel cell vehicles and hybrid vehicles [4]. Compared with these two models, hybrid battery models have been relatively mature. Now, China is vigorously promoting pure electric vehicles. Compared with hybrid vehicles, the core technology of pure electric vehicles is easier to achieve breakthroughs, from the perspective of emissions, it can achieve true zero emissions, clean and pollution-free. However, as the only power source of pure electric vehicles, the power battery pack will generate a lot of heat during charging and discharging, which will cause it to heat up, and then have a greater impact on its internal resistance, voltage, SOC, available capacity, safety and reliability, charging and discharging efficiency and service life and many other thermal physical performance indicators.

With the increase in the use of new energy vehicles, safety accidents of new energy vehicles have become increasingly frequent, and problems such as thermal runaway have become the main cause of fire of new energy vehicles [5]. Therefore, to do a good job of thermal management design for the performance of the battery, life and vehicle indicators are very critical. The main purpose of the thermal management design of the battery pack is to: the heat generated during the charging and discharging of the battery pack, reduce the high temperature of the battery pack caused by a large amount of heat accumulation, and ensure that the battery pack can be charged and discharged normally in the ideal working temperature area; Reduce the overtemperature of the battery in the process of charging and discharging; In order to improve the temperature consistency of the entire battery pack, the temperature difference between the cells in the battery pack is reduced [6].

To sum up, the development of new energy electric vehicles is the only way to sustainable development, how to carry out efficient thermal management of the battery pack, keep the temperature of the battery pack in a suitable range, so as to ensure the service life of the battery pack, charge and discharge performance, safety and stability, which plays a very important role in realizing the efficient and safe operation of electric vehicles.

2. CFD Basic Overview and Thermal Characteristics of Power Batteries

2.1. CFD Basic Overview

In this paper, ANSYS commercial software was used for modeling and simulation analysis, Spaceclaim was used to establish monomer and battery models, and AnSYS-Fluent software was used as calculation software. Computational Fluid Dynamic (CFD) is an analytical method and tool that uses computers to solve fluid flow, heat transfer and related transfer phenomena. CFD is the mathematical discretization of hydrodynamics problems to achieve the analysis of digital and computer simulation. On the basis of computational fluid dynamics and heat transfer, the complicated problems of flow and heat transfer are studied deeply by combining numerical simulation and computer experiment. It greatly replaces the traditional test instrument, saves a lot of development and development cycle, and has great engineering practical value and scientific research value.

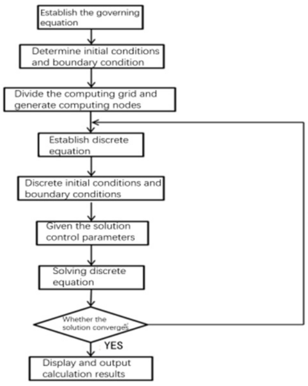

Figure 1. Flowchart of CFD solution

2.2. Heat Generation Mechanism of Lithium-Ion Power Battery

From the working principle of the upper section of the lithium-ion battery to explore the internal heat generation mechanism of the battery, the lithium-ion battery is actually the heat generated by the mutual conversion of chemical energy and internal energy in the process of charging and discharging. The heat production of lithium-ion batteries can be divided into four types [7]: reaction heat, Joule heat, polarization heat, and side reaction heat. Therefore, the total heat generated by lithium-ion batteries Q formula is as follows:

$$Q = Q_r + Q_j + Q_p + Q_s \tag{1}$$

Where: is the heat generated by the electrochemical reaction in the battery. According to the principle of entropy change, the calculation formula of reaction heat is as follows:

$$Q_r = \frac{nmQ_e I}{MF} \tag{2}$$

In the above formula: n - number of cells, m - electrode mass, - electrode reaction heat, I - current, M - molar mass, g/mol, F - Faraday constant.

Ohmic heat, the heat is irreversible, is caused by the internal resistance of the battery itself, in the process of charging and discharging heat, the calculation formula is as follows:

$$Q_j = I^2 R_e \tag{3}$$

Where, -ohmic internal resistance.

The polarization heat is generated because the polarization reaction occurs on the electrode surface of the battery during charging and discharging. In the calculation, a polarization internal resistance is set:

$$Q_p = I^2 R_p \tag{4}$$

The side reaction heat is the heat generated by the side reaction that occurs with the main reaction of the battery, and the side reaction heat is usually very small and is not considered.

2.3. Heat Transfer Characteristics of Lithium-Ion Power Batteries

Because of the internal resistance of the lithium battery itself, when it is charged and discharged, it will produce a lot of heat, which is partly used to do work, partly transmitted to the atmosphere in the form of thermal conductivity, and the other part is absorbed by its own material, so that its temperature rises. The design idea of this paper is: to analyze the influence of natural heat dissipation and liquid cooling system design on the temperature rise of the battery during charging. On the basis of the analysis of natural heat dissipation, the liquid cooling system is used to remove the heat generated by the battery during charging, so as to reduce the use temperature of the battery.

From the basic theory of heat transfer, it can be seen that there are three main ways of heat transfer: heat conduction, heat radiation and heat convection: heat conduction refers to the heat exchange caused by the internal temperature difference or the heat exchange between two contact objects. When the positive and negative electrode materials, membranes, and fluid collectors inside the lithium-ion battery undergo an electrochemical reaction, they generate heat and transfer it to the outer surface of the battery, resulting in heat conduction.

Fourier's law is obeyed, as follows:

$$q_f = -\lambda \frac{\partial T}{\partial n} \tag{5}$$

Where: - heat flux; - Thermal conductivity, W/(m·K); - Temperature gradient, K; "-" indicates transmission to a low temperature.

Heat convection is the process of exchange between itself and the external environment. When the lithium battery is working, the exchange between the outer surface of the battery and the external cooling medium is as follows:

$$q = h_f (T_b - T_f) \tag{6}$$

Where: - heat flux; - convective heat transfer coefficient; - Battery outer surface temperature; - Temperature of the cooling medium.

Thermal radiation is a way of transmitting energy outward in the form of electromagnetic waves. According to the Stefan-Boltzmann law, the expression is as follows:

$$Q_w = \varepsilon\sigma A_1 F_{12} \left(T_1^4 - T_2^4\right) \tag{7}$$

Where: - heat radiates heat; - thermal emissivity; - Steffen-Boltzmann constant; - the area of radiant surface 1; - form factor of radiation; - Absolute temperature of radiant surface 1; - Absolute temperature of radiant surface 2.

From the above three aspects, it can be seen that in the battery pack, when the inner plate of the battery pack performs an electrochemical reaction, the generated heat energy is transferred to the surface of the battery pack through the electrolyte; Heat convection is because there is a certain temperature difference between the electrolytic cell and the outside world. When the liquid flows from the outside surface of the electrolytic cell, the heat energy on the outside surface of the electrolytic cell is exchanged with the outside world by convection heat transfer. The role of thermal radiation is determined by the material and surface temperature of the battery, so the heat dissipation generated is very small, it is difficult to use for heat dissipation, so its role is temporarily ignored.

3. Establishment and Simulation Analysis of Thermal Model of Li-ion battery

3.1. Establishment of Thermal Effect Model of Lithium-ion Battery

According to the characteristics of Li-ion battery, a heat conduction calculation method suitable for Li-ion battery was proposed, and the heat conduction characteristics of Li-ion battery were studied. The second law of thermodynamics: When there is a temperature change between substances, there will be a transformation of energy, there will be heat transfer from a high temperature object to a low temperature object, that is, in the conservation of energy, the transformation of heat cannot transfer a low heat object to a high energy object without causing any effect. In terms of the heat generated by a single battery in the process of charging and discharging, its specific composition is: heat conduction, heat convection and heat radiation. As shown in Figure 2:

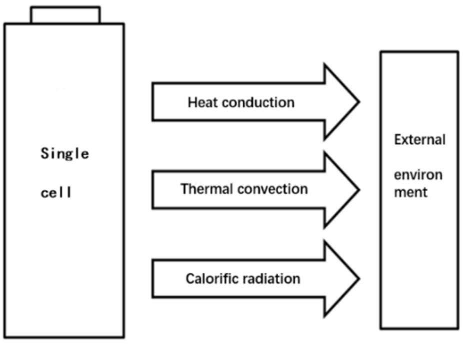

Figure 2. Heat dissipation channels of a battery

Because of the large molecular weight of lithium ions, it is difficult to directly 3D models them. Therefore, the lithium-ion battery studied in this paper makes the following assumptions:

(1) The pseudo-order battery is a homogeneous, heterogeneous, isotropic, and its thermal physical properties are not affected by its own temperature and the external environment;

(2) The electrolyte in the battery is regarded as a whole without liquid flow and convection heat transfer, and only conducts electricity in a separate way;

(3) electrolyte without radiative heat transfer;

(4) The heat generation rate of each component is considered to be equal.

A three-dimensional transient heat transfer mathematical model is established according to the above assumptions, and its energy conservation equation is shown as follows according to the Cartesian coordinate system:

$$\rho_b c_p \frac{\partial T}{\partial t} = k_x \frac{\partial^2 T}{\partial x^2} + k_y \frac{\partial^2 T}{\partial y^2} + k_z \frac{\partial^2 T}{\partial z^2} + q_v \tag{8}$$

Where: - density; b - battery; T- Temperature; - Specific heat capacity; - Thermal conductivity; x, y, z represents three-dimensional coordinates; - Heating rate per unit volume.

The solution of the cell model includes initial conditions and boundary conditions, and its temperature distribution is a function of time and space coordinates.

The initial conditions are:

$$T(x, y, z, 0) = T_0 \tag{9}$$

Where: - Initial temperature.

According to Newton's law, the boundary conditions of the battery are obtained:

$$\begin{cases} -k_x \frac{\partial T}{\partial x} = h(T - T_x) & x = 0, l_b \\ -k_y \frac{\partial T}{\partial y} = h(T - T_y) & y = 0, l_b \\ -k_z \frac{\partial T}{\partial z} = h(T - T_z) & z = 0, l_b \end{cases} \tag{10}$$

3.2. Thermal Performance Parameters of Li-ion Batteries

3.2.1. Determination of Thermal Conductivity of Lithium-ion Battery

The lithium iron phosphate lithium-ion power battery studied in this paper is laminated inside, which is composed of many layers of materials superimposed. The internal figure is shown in Figure 3, and the thermal conductivity can be similar to the method for solving the equivalent resistance.

$$\begin{cases} k_x = \dfrac{l_b}{\sum^i \dfrac{d_{x_i}}{k_i}} = \dfrac{l_b}{\dfrac{d_{x_p}}{k_p} + \dfrac{d_{x_n}}{k_n} + \dfrac{d_{x_s}}{k_s}} \\ k_y = \sum^i \dfrac{k_i d_{y_i}}{b_b} = \dfrac{k_p d_{y_p} + k_n d_{y_n} + k_i d_{y_s}}{b_b} \\ k_z = \sum^i \dfrac{k_i d_{z_i}}{h_b} = \dfrac{k_p d_{y_p} + k_n d_{z_n} + k_i d_{z_s}}{b_b} \end{cases} \tag{11}$$

Where: - Total thickness in three directions in three dimensional coordinates; p, n, s - positive plate, negative plate and diaphragm.

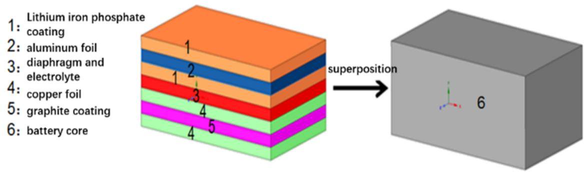

Figure 3. Battery internal layers

3.2.2. Determination of Specific Heat Capacity of Lithium-ion Battery

The specific heat of each component was obtained by the component analysis, and the average was obtained by the gravimetric method.

According to the assumptions of the battery thermal effect model, the internal and external components of the battery were analyzed, and the specific heat capacity of the battery was calculated by using the weighting method [8]:

$$c_p = \frac{1}{m_b} \sum_i c_i m_i \tag{12}$$

Where: - specific heat capacity of the battery, - specific heat capacity of the material, - mass of the material, - mass of the battery cell.

3.2.3. Heat Generation Rate of Lithium-ion Batteries

In the chamber heat condition, when the lithium-ion battery is in the working state, its internal resistance is only a small change, can be ignored; In other words: in the absence of charging and discharging, the internal resistance of the battery has not significantly changed. Because we only investigated the ambient temperature in summer, and no charging and discharging occurred under simulated conditions, we assumed that the internal resistance of this lithium iron phosphate battery was constant.

According to the battery thermal model theory [10] established by Bernardi [9], the formula is as follows:

$$\phi = I\left[\left(E_0 - E\right) - IT\frac{\partial E_0}{\partial T}\right] \tag{13}$$

Where: - heat generation power; - Current; - open circuit voltage; - Load voltage; - Temperature.

Through the above theoretical analysis, assuming that the DC internal resistance of the battery does not change with the change of current and temperature, the following equation is obtained:

$$E_0 - E = I \cdot R_t \tag{14}$$

Sorting out the above two equations can be obtained:

$$\phi = I^2 R_t - IT\frac{\partial E_0}{\partial T} \tag{15}$$

Where: is the internal resistance of lithium-ion power battery; It is determined by the chemical reaction, and the calculated value is very small, less than 2% of the total heat, so it can be ignored.

Therefore, the total heat of the power battery can be calculated as:

$$\phi = I^2 R_t \tag{16}$$

Through software Settings, set the calorific value per unit volume in Fluent, the unit is W/m3, and the calculation formula is as follows:

$$q_v = \frac{\phi}{V} = \frac{I^2 R_t}{V} \tag{17}$$

The thermophysical parameters of the lithium-ion power battery studied in this paper are shown in the figure 4 provided by a battery factory.

Figure 4. Actual battery

Table 1. Performance parameters of lithium-ion power batteries

Serial number	Item	Specification
1	Battery type	Lithium iron phosphate battery
2	Battery type	LP40190200—80Ah
3	dimension	40mm*190mm*200mm
4	weight	3.18±0.1kg
5	Operating voltage	2.5V~3.65V
6	Operating temperature range	-30℃~60℃
7	Optimum operating temperature range	15℃~35℃
8	Specific heat capacity	1180（J/kg-k）
9	Dc internal resistance	<1.5mΩ

The following research object is lithium iron phosphate battery, which specifically describes the performance parameters of lithium iron phosphate battery, such as: battery model, size, weight, operating voltage, etc. Table 1 lists the specific values.

3.3. Simulation Analysis of Single Lithium-ion Battery

This section studies the internal temperature field distribution and temperature rise of lithium iron phosphate battery under natural convection at different discharge rates of 1C, 2C and 3C.

This paper uses Ansys SCDM drawing software to establish a three-dimensional model of a single battery. The length × width × height of a single battery is 200mm× 40mm × 190mm. The three-dimensional model is shown in Figure 5 below.

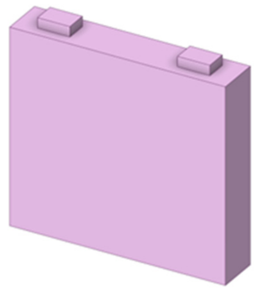

Figure 5. Three-dimensional battery model

A single 3D model was introduced into ANSYS mesh software. Due to the regular appearance and small size of the battery model, tetrahedral mesh division was used in this paper, and a total of 614,679 grids and 117,685 nodes were divided. In the grid division, most of the units are high-quality units, only a few inferior units, so the calculation will not have any impact on the accuracy and reliability of the calculation results. The grid model of a single cell is shown in Figure 6:

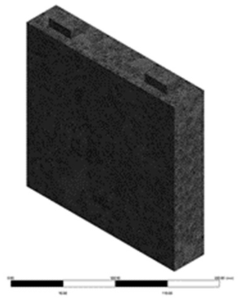

Figure 6. Battery grid division

In this section, the temperature distribution of square lithium-ion batteries of pure electric vehicles under the state of natural air convection is studied, and the temperature rise of the battery under different discharge rates of 1C, 2C and 3C is observed. The initial temperature of the battery is set to 25℃, and the air convection coefficient is set to 5w/ (m2*k).

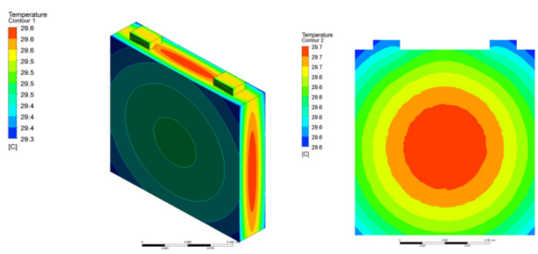

Figure 7. Overall discharge and cross section of the 1C battery

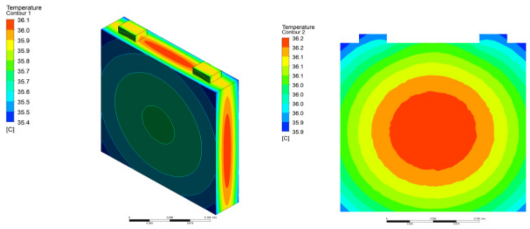

Figure 8. Battery 2C discharge overall and cross section cloud view

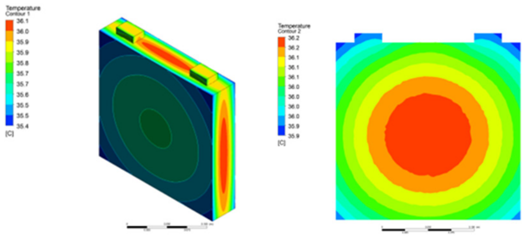

Figure 9. Battery 3C discharge and cross section cloud view

As can be seen from the above temperature field cloud map, the temperature of the central section of the single battery after the discharge is the highest and decreases around the edge of the battery, mainly because the heat is generated inside the battery, and the external ambient temperature is 25℃, the air convection coefficient is 5w/m2-k, and some heat is dissipated into the air. The simulation results of temperature field of single battery also show that the greater the discharge current, the greater the internal heat of the battery and the greater the temperature rise of the battery.

As can be seen from the simulation results, when 1 C, 2 C, 3 C. At 1 C, the maximum surface temperature of the electrode is 29.6℃, at 2 C, the maximum surface temperature of the electrode is 36.1℃, and at 3C, it is 43.5℃. With the increase of discharge rate, the temperature rise of single battery also increases.

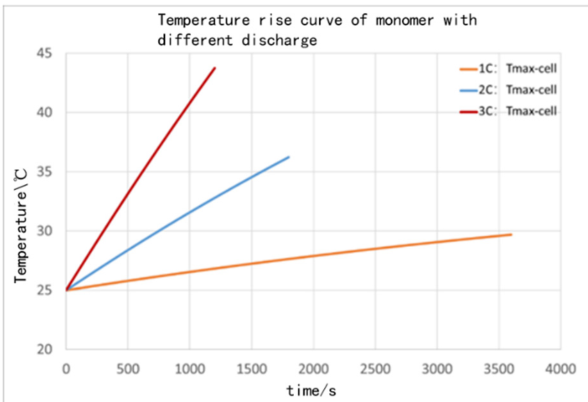

Figure 10. Temperature rises curve of monomer with different discharge rates

As can be seen from the temperature rise curve in Figure 10, the temperature rise of the battery is determined by the discharge current during the discharge of 100~0%SOC, and the discharge rate of the battery is directly proportional to the temperature rise rate.

4. Battery Pack Liquid Cooling Scheme Design

4.1. Scheme Design of Liquid Cooling Pipeline

The battery pack consists of six cells. Each cell is a unit. 2mm foam is placed between each group. The end plate and side plate of the module are made of aluminum for heat dissipation. The liquid cooling pipe is designed at the bottom of the module, and the inlet and outlet are set as circular pipes with A diameter of 10mm, the liquid thickness in the flow channel is 2mm, and the width of each flow channel is 4mm. Scheme A is type I flow channel, and scheme B is type S flow channel, which relies on the circulation of coolant in the liquid cooling system to carry away the heat generated by the battery, so as to achieve the purpose of heat dissipation, as shown in Figure 11 and 12.

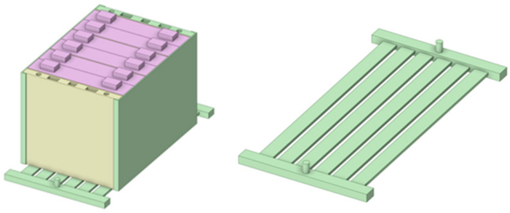

Figure 11. Solution A: Model I liquid cooled battery string design

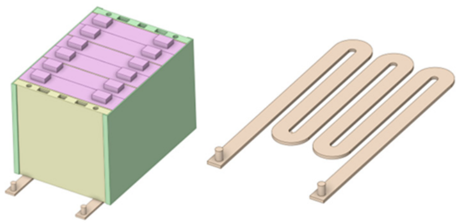

Figure 12. Solution B: S-type liquid cooled battery string design model

4.2. Comparison of Different Liquid Cooling Schemes

4.2.1. Liquid Cooled Battery Pack Meshing

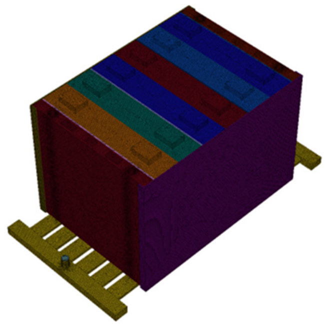

Figure 13. Grid division of the type I liquid cooled battery string

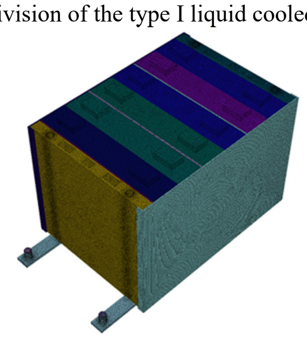

Figure 14. Grids of S-type liquid cooled battery strings

In order to avoid errors in calculation accuracy caused by different mesh size Settings, the mesh size is set to soft command 2mm. In calculation, tetrahedral mesh division is adopted to improve simulation accuracy, and boundary layer of fluid domain is set to 2 layers. A total of 2529840 grids are divided into scheme A and 2509053 grids are divided into scheme B. The maximum skew slope of grid quality is 0.84 and 0.85, respectively. Most of the units in grid division are high-quality units, and only a small number of low-quality units, which will not affect the accuracy and reliability of the calculation results. Figure 13.and 14. show the grid.

4.2.2. Comparison of Heat Dissipation Effect of Different Liquid Cooling Schemes

The inlet temperature of the liquid cooling pipeline is set at 20℃, the flow rate is 1m/s, the initial temperature of the battery is 25℃ in the normal temperature environment, and the cooling medium is ethylene glycol (a mixture of 50% water and ethylene glycol). The heat dissipation effect under the discharge rate of 1C, 2C and 3C is compared, as shown in the simulation cloud image 4.5~4.10:

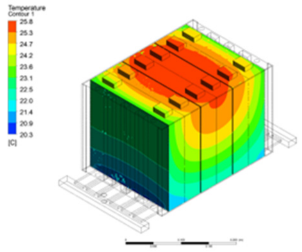

Figure 15. Temperature cloud diagram of the I-1C battery pack

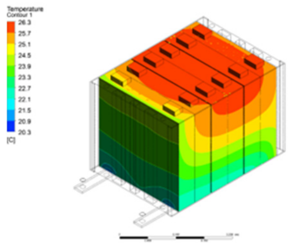

Figure 16. Temperature cloud diagram of the S-1C battery pack

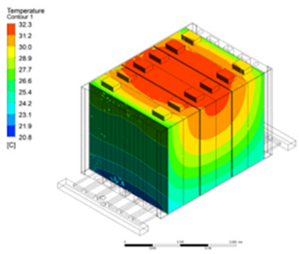

Figure 17. Temperature cloud image of the I-2C discharge battery pack

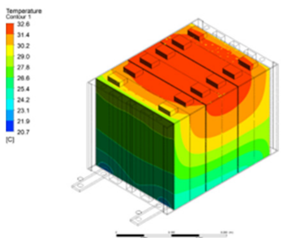

Figure 18. Temperature cloud image of the S-2C discharge battery pack

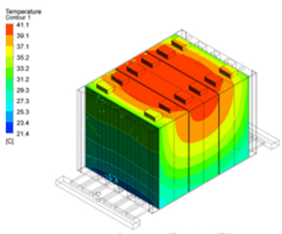

Figure 19. Temperature cloud image of the I-3C discharge battery pack

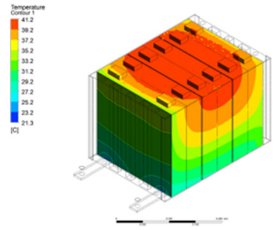

Figure 20. Temperature cloud image of the S-3C discharge battery pack

Through simulation analysis, it can be seen that the I-type liquid cooled battery pack and S-type liquid cooled battery pack are similar in the cloud image. The highest temperature in the battery pack is mainly concentrated in the middle area of the upper end of the battery pack, and the temperature at the bottom of the battery pack is low, mainly due to the low temperature of the coolant in the liquid cooled pipe. While the battery pack generates heat, part of the heat is dissipated through the liquid cooled pipe. Therefore, the battery pack temperature near the liquid cooling pipe is low, and the battery pack temperature far away from the liquid cooling pipe is high. Figure 21. shows the temperature rise curves of the two solutions under different working conditions, and Table 2. lists the data.

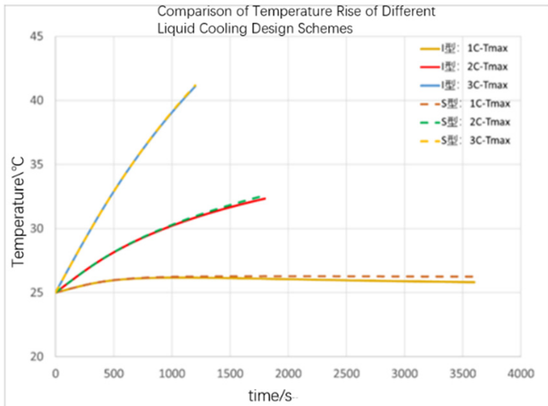

Figure 21. Temperature rise curve

For two different liquid cooling designs, the same discharge rate is compared and analyzed. From the temperature rise curve, it can be seen that the maximum temperature curve of the S-type liquid cooling design is slightly higher than that of the I-type liquid cooling design. (Data source)

Table 2. Temperature rise comparison between the I liquid cooled battery string and the S liquid cooled battery string

Discharge condition	Type I Tmax-Cell	Type S Tmax-Cell	S-I=△T
1C	25.8	26.3	0.5
2C	32.3	32.6	0.3
4C	41.1	41.2	0.1

Through analysis and comparison, under different discharge ratios, the maximum temperature of the type I liquid cooled battery pack is lower than the maximum temperature of the type S. The main reason is that the coolant of the type I flow channel flows from one end of the battery pack to the other end during the flow process, and the temperature difference between the coolant and the battery pack is large, and the heat dissipation efficiency is high. The coolant in the S-channel flows into the end of the battery pack from a section, and the coolant keeps absorbing heat, resulting in a rise in temperature, and the temperature difference with the battery pack reduces the heat dissipation efficiency. Therefore, in the analysis and comparison, the cooling effect of the I-channel is considered to be the best.

5. Optimization Analysis of Liquid Cooling Design of Battery Pack

This chapter designs two types of liquid cooling battery packs, type I and Type S. By setting the same liquid cooling control strategy, the inlet temperature is 20℃, the flow rate is 1m/s, the initial temperature of the battery is 25℃ in normal temperature environment, and the cooling medium is glycol (50% water and glycol mixture). Through the simulation analysis and comparison of the heat dissipation effect under the three discharge rates of 1C, 2C and 3C, the maximum temperature of the type I liquid cooled battery pack is lower than that of the type S liquid cooled battery pack.

5.1. Effect of Coolant Flow Rate on Heat Dissipation of Battery Pack

Based on the analysis of heat dissipation of battery packs with different charging rates by cooling channel in the previous chapter, the S-type liquid cooled battery pack design scheme will be adopted to analyze the influence of different inlet flow rates on heat dissipation of battery packs. Considering that the best operating temperature range of the battery is 15℃~35℃, the discharge ratio is based on 2C, and the initial temperature of the battery is set at 25℃ and the inlet temperature is 20℃. The influence of the inlet flow rate of 0.5m/s, 1m/s, 1.5m/ s and 2m/s on the heat dissipation of the battery pack is analyzed. The simulation results are shown in Figure 22 to 25.

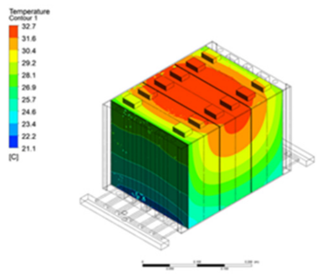

Figure 22. Temperature cloud diagram at a velocity of 0.5m/s

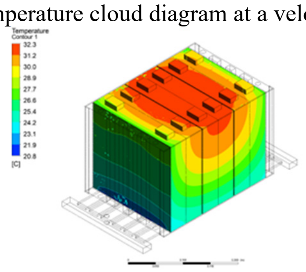

Figure 23. Temperature cloud diagram at a velocity of 1m/s

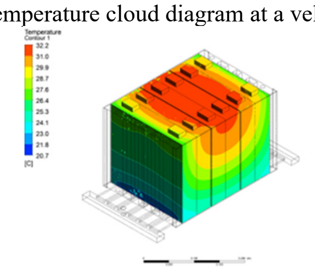

Figure 24. Temperature cloud diagram at a velocity of 1.5m/s

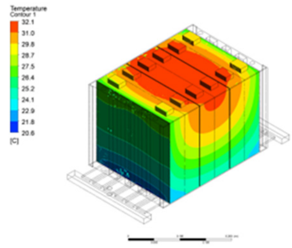

Figure 25. Temperature cloud diagram at a velocity of 2m/s

Based on the analysis software Fluent, the inlet flow of the liquid cooling system with different 2C charging ratios was simulated and analyzed. Under the condition that the flow rate was 0.5m/s, the highest temperature of the battery pack was 32.7℃, and the lowest temperature was 21.1℃. Under the condition of flow rate of 1m/s, the maximum temperature of the battery pack is 32.3℃, and the minimum temperature is 20.8℃. Under the condition of flow rate of 1.5m/s, the maximum temperature of the battery pack is 32.2℃, and the minimum temperature is 20.7℃. Under the condition of flow rate of 2m/s, the maximum temperature of the battery pack is 32.1℃ and the minimum temperature is 20.6℃. According to the above data analysis, the maximum temperature rise in the discharge process of the battery pack is 32.7℃, 32.3℃, 32.2℃ and 32.1℃ respectively. It can be seen that simply increasing the flow rate has little effect on the heat dissipation effect of the battery pack.

5.2. Effect of Coolant Temperature on Heat Dissipation of Battery Pack

The previous chapter mainly analyzed the influence of different coolant flow rates on the heat dissipation of the battery pack. This section analyzed the influence of water temperature on the heat dissipation of the battery pack by changing the inlet temperature of the coolant. With the inlet flow rate of 1m/s as the quantification, the initial temperature of the battery is set to 25℃, and the temperature of the coolant is set to 16℃, 18℃, 20℃, and 22℃ respectively. The calculation results are shown in Figure 26~29:

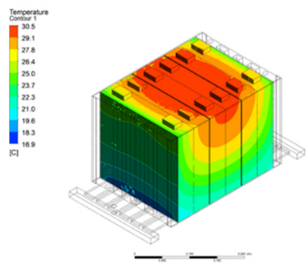

Figure 26. Coolant 16 ° C battery pack temperature cloud diagram

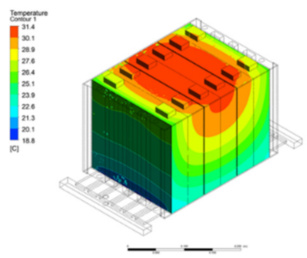

Figure 27. coolant 18 ° C battery pack temperature cloud diagram

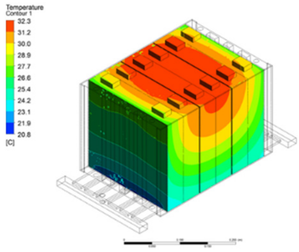

Figure 28. Coolant 20 ° C battery pack temperature cloud diagram

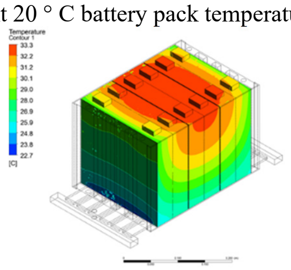

Figure 29. coolant 22 ° C battery pack temperature cloud diagram

Based on the analysis software Fluent, the liquid cooling system is simulated with 2 C charging rate and different flow channel widths: in the cooling medium of 16℃, the highest temperature of the battery stack reaches 30.5℃, while the lowest temperature of the battery stack reaches 16.9℃. When the coolant temperature is 18℃, the maximum and minimum operating temperatures of the battery stack are 31.4℃ and 18.8℃ respectively. When the coolant temperature is 20℃, the maximum and minimum of the battery stack are 32.3℃ and 20.8℃ respectively. When the coolant temperature is 22℃, the maximum and minimum of the battery stack are 33.3℃ and 22.7℃, respectively. According to the above data, the maximum temperature rise in the discharge process of the battery pack is 30.5 ℃, 31.4 ℃, 32.3 ℃ and 33.3 ℃ respectively. It can be seen that the maximum temperature of the battery pack will drop by 1℃ for every 2℃ reduction in the coolant inlet temperature.

Figure 30 shows the temperature rise curve of the battery string:

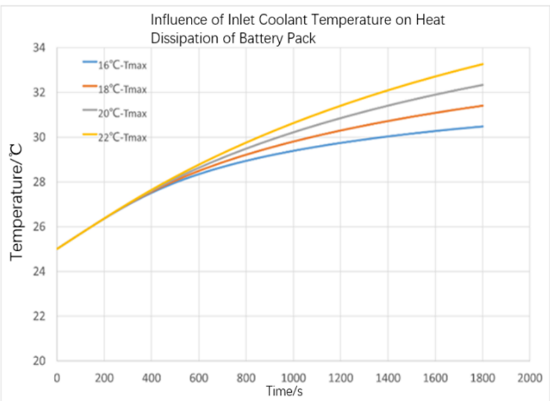

Figure 30. Temperature rises curves of battery strings with different coolant temperatures

It can be seen from the temperature rise curve that the temperature rises rate of the battery pack for the first 400s is consistent with different inlet temperature, that is, the maximum temperature of the battery pack is the same. With the increase of time, the different inlet temperature plays a role in the heat dissipation of the battery pack after 400s, and the heating rate decreases with low water temperature. Therefore, it can be concluded that, the heating rate of the battery pack is directly proportional to the water inlet temperature of the liquid cooling system.

6. Conclusion

This paper takes lithium-ion battery as the object, focuses on the key scientific problem of its temperature rise in the process of charge and discharge, conducts in-depth theoretical analysis from the aspects of structure composition, working principle, heat production mechanism and heat exchange characteristics, builds its thermal effect mathematical model, and determines its thermal physical performance indicators. Based on this, Fluent software is used in this paper to conduct numerical simulation of the monomer and water-cooling system of the system, and the following results are obtained:

(1) Under the condition of 25℃, a single lithium battery is simulated by thermal model with three different discharge rates of 1 C, 2 C and 3 C. The results show that the maximum temperature of the electrode surface during the discharge period is 29.6℃, 36.1℃ and 43.5℃, respectively. When the charge and discharge rate increases, the maximum operating temperature will increase significantly, and the discharge rate of the battery is directly proportional to the temperature rise.

(2) Two liquid cooled type I and type S liquid cooled battery packs are designed. Under the same liquid cooling mode, the same liquid cooling mode is adopted, the inlet water temperature is 20℃, the water flow rate is 1m/s, and the initial temperature of the battery is 25℃ under room temperature conditions. Glycol (containing 50% water and glycol mixed solution) is used as the cooling medium. Through simulation and comparison, the highest temperature of type I liquid cooled battery pack is lower than that of type S liquid cooled battery pack at three different discharge rates of 1 C, 2 C and 3 C.

(3) According to the theory of type I and the theory of control variables, the calculation results under the conditions of various cooling media flow and inlet temperature are simulated and calculated. The results show that increasing the coolant flow rate has no obvious effect on the thermal radiation efficiency in the reactor. At the same time, as the coolant inlet temperature drops, the maximum temperature of the battery stack also drops.

Acknowledgments

Thanks to the Sichuan Mineral Resources Research Center, which has set up a project: Research on the Recovery and Utilization of Secondary Mineral Recycling in the Battery of New Energy Vehicles, project number: SCKCZY2023-ZC009; The project of "Chengdu Research Center for Integrating into a New Pattern of Dual Cycle Development" and "Sichuan Research Center for Integrating into a New Pattern of Dual Cycle Development" is based on the development strategy research of Sichuan's integration into the dual cycle new energy vehicle industry under the background of "dual carbon". Project number: SXHY20022jl002; Support for this article from the Geely University Teaching and Research Training Project, Geely University Brand Curriculum Construction Project, and the New Energy Vehicle Power Battery Control Technology Innovation Platform.

References

[1] Hu Hua, Song Hui. Electric vehicles [C]. People's Communications Press, 2003:161-162.

[2] Chen Qingzhi, You Yi. Application status and development trend of new energy vehicle power battery [J]. Times Automobile, 2021, (09) : 107-108+111.

[3] Zhu Liqi. China: From automobile power to automobile power [J]. Qicai Language, 2022, (34) : 2-5.

[4] Ran Ailing. Research on the development of new Energy Vehicles and power lithium Batteries [J]. Automotive Practical Technology, 2019, 12 (2) : 13-14.

[5] Chen Xiaoping. Review on safety technology of new energy vehicle power battery [J]. Science and Technology Today, 2020, (11) : 49-51.

[6] Kim J, Oh J, Lee H.Review on battery thermal management system for electric vehicles[J]. Applied Thermal Engineering, 2019, 149:192-212.

[7] Zhang Guoqing, Ma Li, Zhang Haiyan. Heat production behavior and thermal management technology of HHV batteries [J]. Journal of Guangdong University of Technology, 2008, (01):1-4.

[8] Liu Feifei, LAN Fengchong, Chen Jiqing. Simulation and test of Temperature field of Automotive lithium-ion power Battery based on Dynamic internal heat source [J]. Journal of Mechanical Engineering,2016,(08)141-151.

[9] Nagpure S C, Dinwiddie R., Babu S. S. Thermal diffusivity study of aged Li-ion batteries using flash method[J]. Journal of Power Sources, 2010, 195(3): 872-876.

[10] Bernardi D, Pawlikowski E, Newman J. A general energy, balance for battery systems[J]. Journal of the Electrochemical Society, 1985, (1).